Asian Journal of Applied Science and Technology (AJAST)
Volume 5, Issue 4, Pages 69-81, Oct-Dec 2021

Plant Mediated Synthesis of ZnO and Mn Doped ZnO Nanoparticles Using Carica Papaya Leaf Extract for Antibacterial Applications

N. Priyadharsini[1*], N. Bhuvaneswari[2] & Jomin Joshy[1]

[1]*Department of Physics, Dr. N.G.P Arts and Science College, Coimbatore-641048, Tamilnadu, India.*
[2]*Department of Physics, Rathinam College of Arts and Science, Coimbatore- 641021, Tamilnadu, India.*

DOI: http://doi.org/10.38177/ajast.2021.5409

Article Received: 25 September 2021 *Article Accepted: 21 November 2021* *Article Published: 19 December 2021*

ABSTRACT

In this work, Zinc Oxide (ZnO) and Mn-doped ZnO nanoparticles were green synthesized using Carica papaya extract by the Co-precipitation method. X-ray diffraction (XRD) results revealed the formation of ZnO and Mn-doped ZnO nanoparticles with the wurtzite crystal structure (hexagonal). Due to the presence of dopant Manganese (Mn) the optical spectra showed a redshift in the absorbance spectrum. Structural and optical properties of the end product showed that the manganese ions (Mn^{2+}) substituted the Zinc ions (Zn^{2+}) without altering the Wurtzite structure of ZnO. Fourier Transform Infrared Spectroscopy (FTIR) spectra confirm the presence of metal oxide present in the end product. The antibacterial efficiency of ZnO and Mn-doped ZnO nanoparticles were studied using the agar well diffusion method against Gram-positive and Gram–negative bacteria. It is obvious from the results that Mn doped ZnO nanoparticles exhibit better antibacterial activity than ZnO nanoparticles.

Keywords: Carica papaya, X-ray diffraction, Optical properties, Anti-bacterial activity.

1. Introduction

Nanotechnology is one of the rapidly developing concepts in the field of Science and Technology [1]. Nanoparticles acquire much importance due to their excellent chemical and thermal stability [2]. Physical, chemical, electrical and optical properties have a significant role in the size and shape of the nanomaterials. [3],[4],[19]. Zinc oxide is an inorganic material, classified as a semiconductor in group II-VI. It has a broad energy band gap of 3.37 eV, high binding energy of 60 meV [5].

ZnO has unique optical and chemical behaviors which can be easily reformed [6]. ZnO nanoparticles have a tremendous potential application in Ultra- violet lasers, piezoelectric transducers, dye-sensitized solar cells and biological applications such as biosensors, bioimaging, drug delivery, biological sensing, biological labeling, gene delivery, drug delivery and Nano medicine along with its antibacterial, antifungal and anti-diabetic activities [6]-[9],[21]-[23]. Lower cost, UV blocking properties, high catalytic activity, large surface area are the advantages of nanostructured ZnO particles compared to other metal nanoparticles [7],[24].

Synthesis of nanoparticles via green routes has become popular among researchers due to its low cost, clean, safe, synthesis in ambient atmosphere, non-toxicity, environmental compatibility etc. [2],[7],[10]. Nanoparticles are bio-synthesized directly from metal or metal salts, in the presence of some organic material or plant extract [4],[18]. The use of plants and/or plant leaf extract offers a biological method for the controlled and precise synthesis of several metallic nanoparticles with well-defined diverse sizes and shapes [7],[20]. The properties of the semiconductor such as band gap or electrical conductivity can be controlled by doping a selective element into ZnO. Furthermore, an increase in surface area and decrease in particle size can be done by doping transition metals such as Manganese, Chromium, Nickel, Cobalt into ZnO [10],[11]. Carica papaya originated from the low lands of eastern Central America is also known as papaya or paw-paw. It has been widely cultivated in tropical countries for

its edible fruit for hundreds of years and has also been used in traditional ethnic health applications [12]. Phenolic compounds, alkaloids, glycosides, amino acids, antioxidant vitamins and minerals were the constituents of the extracts of Carica Papaya which may be responsible for their observed antioxidant activities [25],[26]. Alkaloids have established broad-spectrum antibacterial activity and are also used as analgesics and narcotics for pain relief [13]. In the present work, we report simple, efficient and cost-effective green synthesis of ZnO and Mn doped ZnO nanoparticles using Carica papaya leaf extract which acts as a reducing and capping agent. The purpose of this work was to compare the performance of biosynthesized ZnO and Mn-doped ZnO nanoparticles for better antibacterial activity using the co-precipitation method.

2. Experimental methods

2.1. Materials

Pure and Manganese doped zinc oxide nanoparticles were synthesized by Co-Precipitation method. All the analytical reagents were obtained from Merck Chemicals and used without further purification. Zinc nitrate hexahydrate ($Zn(NO_3)_2.6H_2O$) was used as a host precursor, manganese acetate hexahydrate ($Mn(CH_3COO)_2.4H_2O$) was used as dopant precursor. Sodium hydroxide (NaOH), Plant extract and de-ionized water were used in precursor solutions.

2.2. Preparation of Plant Extract

Fresh leaves of Carica Papaya were collected from fields, near Dr. N.G.P Arts and Science College, Coimbatore, India. The leaves were thoroughly washed for 2-3 times with double distilled water and dried at room temperature. 5 g of Carica papaya leaves was added to 100 mL of distilled water and was heated for 60 min in 100°c. Then Papaya leaf extract was filtrated using Whatman paper no.1 and the extract was stored for further studies.

2.3. Synthesis of Zinc Oxide Nanoparticles

ZnO nanoparticles have been prepared using the required precursors by Co precipitation method. An aqueous solution of 1 M Zinc nitrate hexahydrate ($Zn(NO_3)_2.6H_2O$) was dissolved in 100 mL double distilled water (DDW) and stirred for about 15 minutes at room temperature. In the above solution, add 20 mL of plant extract (5:1) to aqueous solution drop wise and stirred again for 15 minutes.

Later, 1 M Sodium hydroxide (NaOH) was dissolved in 100 mL double distilled water and the solution was stirred for 15 minutes. Finally, the NaOH solution was added to the above solution and continuously stirred for 1 hour at room temperature.

After 1 hour, the deposited white precipitate is centrifuged and washed with distilled water and ethanol several times. After centrifugation (3000 rpm), the samples were dried in hot plate at 100°C for 2 hours. Then, the prepared ZnO nanoparticles are powdered using mortar and stored for further studies.

2.4. Synthesis of Mn doped Zinc Oxide nanoparticles

Mn doped ZnO nanoparticles have been prepared using Co precipitation method. Initially, an aqueous solution of 1M Zinc nitrate hexahydrate ($Zn(NO_3)_2.6H_2O$) was dissolved in 100 mL double distilled water (DDW) to which 5

wt% of Manganeous acetate was added and stirred for 15 minutes. Then 20 mL of plant extract (5:1) was mixed to it and stirred again for next 15 minutes. Secondly, 1M Sodium hydroxide (NaOH) was dissolved in 100 mL double distilled water and stirred for another 15 minutes. Finally, the NaOH solution was added to the above solution and continuously stirred for 1 hour at room temperature. After 1 hour, the deposited white precipitate is centrifuged and washed with distilled water and ethanol several times. After centrifugation (3000 rpm), the samples were dried in hot plate at 100°C for 2 hours. Then, the prepared ZnO nanoparticles are powdered using mortar and stored for further studies.

2.5. Characterization

The synthesized ZnO nanoparticles were characterized using various spectroscopic techniques. Structural properties such as crystalline structure, average crystalline size, cell parameters, and phase identification were analyzed using X-ray diffractometer. Optical properties were analyzed using UV and FTIR techniques. UV–visible spectrum was recorded between 200 and 800 nm using UV–Visible spectrophotometer. Fourier transform infrared (FTIR) analysis of the nanoparticles was carried out with Fourier transform spectrometer at a frequency range of 4000-400 cm^{-1}.

2.6. Evaluation of Antibacterial Activity

The anti-bacterial activity of pure ZnO and Mn doped ZnO (5 wt.%) were tested against each Gram-positive and Gram-negative pathogenic such as *Staphylococcus aureus* and *Escherichia coli* respectively. Anti-bacterial activity of nanoparticles was determined by agar well diffusion method. The bacterial suspension was seeded on MHA (Muller Hinton Agar) plates. The nutrient broth culture medium was prepared which is then sterilized in an autoclave at 120°C for an hour. The ZnO and Mn doped ZnO nanoparticles of 0.015g (15 µL) are dissolved in 1mL of DSMO (dimethyl sulfoxide). The cultures of the bacteria were inoculated in 100mL of the nutrient broth and incubated for 24 hours at 37°C. The medium was transferred into the petriplate; once it solidifies the inoculated pathogenic was swabbed around the medium to allow growth using a loop. In each of these plates four wells were cut out using a sterilize cork borer. Using a micro pipette, 100 µL of different concentrations (25µL, 50µL and 75 µL) of nanoparticles and negative control was added in to different wells. A positive control antibiotic disc was placed in the plate and kept in the incubator at 37°C for 24 hours. A positive control without the test sample was also observed. Finally, the antibacterial activities were studied by measuring the diameter around the undoped and doped ZnO nanoparticles. The diameters of the inhibition zones were measured by using millimeter scale.

3. Results and Discussion

3.1. XRD Analysis

Fig.1 shows the X-ray diffraction patterns of the green synthesized and Mn doped ZnO (5 wt%) with Carica Papaya extract nanoparticles by Co-precipitation method. The obtained diffraction peaks are well indexed with JCPDS card no. 36-1451. The sharp and intense peaks indicate that samples are highly crystalline and confirm the hexagonal wurtzite structure of ZnO with lattice parameter a = 3.187 Å and c = 5.258 Å. The growth of nanoparticles has taken place along the easy direction of crystallization of ZnO, which can be confirmed by the

high intensity (1 0 1) peak [14]. The prominent peak of undoped ZnO is 36.59 whereas in the case of Mn doped ZnO is 32.51. The formation of small-sized particles can be confirmed from the broadening of the peak. The diffraction peaks of Mn doped sample show a small shift towards larger and smaller angles when compared to ZnO.

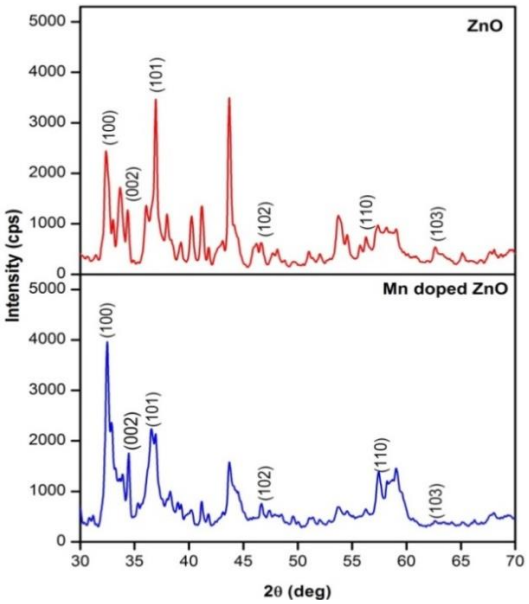

Fig.1. The XRD pattern of Carica Papaya extract ZnO and Mn doped ZnO

The crystalline size of ZnO and Mn doped ZnO can be calculated using Debye-Scherrer equation (D).

$$D = \frac{k\lambda}{\beta_D \cos(\theta)} \qquad (1)$$

Where, D - Crystalline size, K – Shape factor (0.89), λ – Wavelength of Incident radiation, β_D – peak width in Full Width Half Maxima, Θ - Diffraction angle.

The average grain size of un doped ZnO is 7.75 nm and Mn doped ZnO is 8.48 nm. The crystalline size of ZnO nanoparticles increases with the increase in concentration of Mn. Table 1 exhibits the relation of crystalline size of ZnO and Mn doped ZnO nanoparticles. Increase of crystalline size due to the presence of dopant (Mn) which may be due to less solubility of Mn in ZnO.

The diffraction peaks at 2θ (degrees) – 32.42°, 34.09°, 36.59°, 46.55° and 56.19° are respectively indexed to (1 0 0), (0 0 2), (1 0 1), (1 0 2) and (1 1 0) planes of ZnO. These miller indices are in good accordance with JCPDS card no. 36-1451 (Lattice: Primitive, Space group: $P6_3mc$ [186]).

The lattice parameters '*a*' and '*c*' can be calculated from (1 0 0), (0 0 2) peaks using the Eq.2. Calculated lattice parameters are almost similar to JCPDS card No.36-1451 value of ZnO. The presence of Mn causes a slight variation in lattice parameters. This variation may be accounted for the fact that ionic radius of Zn^{2+} (0.60) is smaller than that of Mn^{2+} (0.66).

$$\frac{1}{d^2} = \frac{4}{3}\left[\frac{h^2+hk+k^2}{a^2}\right] + \frac{l^2}{c^2} \qquad (2)$$

Where, d – Interplanar distance, h,k,l – Miller indices, a, c – lattice Constant.

Table 1. Crystalline size and Lattice parameters of ZnO and Mn doped ZnO

Sample	Crystalline Size (nm)	Lattice Parameters		c/a ratio
		a (Å)	c(Å)	
ZnO	7.75	3.187±0.062	5.258±0.052	1.650±0.048
Mn doped ZnO (5 wt%)	8.48	3.189±0.06	5.358±0.152	1.685±0.083

The same results were also reported in Rekha et al. [14]. Table 2 shows that dislocation density (δ) and bond length *(l)* increases with the presence of dopant (Mn) while Micro-strain (ε) and APF (%) decreases. The slight shift of the XRD peaks with the Mn doped ZnO represents that Mn has been effectively doped into the ZnO host structure at the Zn site. Some impurities are observed which may due to excess oxide content and impurities present in plant extract. The average Dislocation density (δ) is determined by using Williamson Smallmann equation, which only depends upon crystalline size (D),

$$\delta = \frac{1}{D^2} \qquad (3)$$

The volume of the obtained nanoparticles (V) can be calculated using the formula,

$$V = \frac{4}{3}\pi\left(\frac{D}{2}\right)^3 \qquad (4)$$

Then the volume of the ZnO and Mn doped ZnO unit cell (v) also has been determined using the equation,

$$v = \frac{\sqrt{3}}{2}a^2c \qquad (5)$$

From the volume of the unit cell and the volume of the crystallite, we can estimate the number of unit cells per crystallite (n) using the equation,

$$n = \frac{V}{v} = 0.6043\left(\frac{D^3}{a^2c}\right) \qquad (6)$$

Where, n – number of unit cell, V – Volume of Unit cell, v – Volume of crystallite.

The estimated values in Table 2 clearly showed that the increase in number of unit cells per crystallite. The estimation of ZnO bond length (*l*) is another way of confirming the presence of dopant. The following relation will estimate the bond length '*l*' of ZnO and Mn doped ZnO,

$$l = \sqrt{0.3a^2} \qquad (7)$$

Bond length has been found to 1.7456 Å for Zn-O and it increases to 1.7467 Å for 5 wt% Mn doped ZnO, which also confirms the substitution of Mn^{2+} in ZnO matrix. Furthermore, the intensities of all diffraction peaks are similar which indicates that the growth of ZnO and Mn doped ZnO in all the planes are same and isotropic [8]. The values of APF are listed in Table 2 and it can be determined using the Eq.8. Approximately 74 % is the APF of bulk

hexagonal ZnO material but in our case the APF of ZnO and Mn-doped ZnO nanoparticles is found to be nearly 73.29 % and 71.74%, respectively. It means that APF in nano crystals are slightly smaller than that of bulk materials due to less solubility of Mn in ZnO. Atomic Packing Factor can also be calculated using the formula,

$$\text{APF}\ (\%) = \frac{2\pi a}{3\sqrt{3}c} * 100 \qquad (8)$$

Table 2. Additional parameters of ZnO and Mn doped ZnO

Sample	Volume of the particles V $(nm)^3$	Volume of the unit cell v $(Å^3)$	No. of unit cells n=V/v	Dislocation density 'δ' $(x10^{16})$	Micro-Strain 'ε' $(x10^{-4})$	Bond length '*l*' (Å)	APF (%)
ZnO	243.7270	46.25±1.37	5.2699	1.8709	51.8266	1.7456	73.29
Mn doped ZnO (5wt%)	320.3091	47.19±0.43	6.7877	2.3743	48.0731	1.7467	71.74

3.2. UV - Vis Spectroscopy

Fig.2 shows the UV – Vis spectra of ZnO and Mn doped ZnO with Carica Papaya extract. The ZnO exhibit's its absorption peak at 360 nm and Mn doped exhibit's absorption peak at 364 nm with band gap of 3.451 eV and 3.413 eV, respectively.

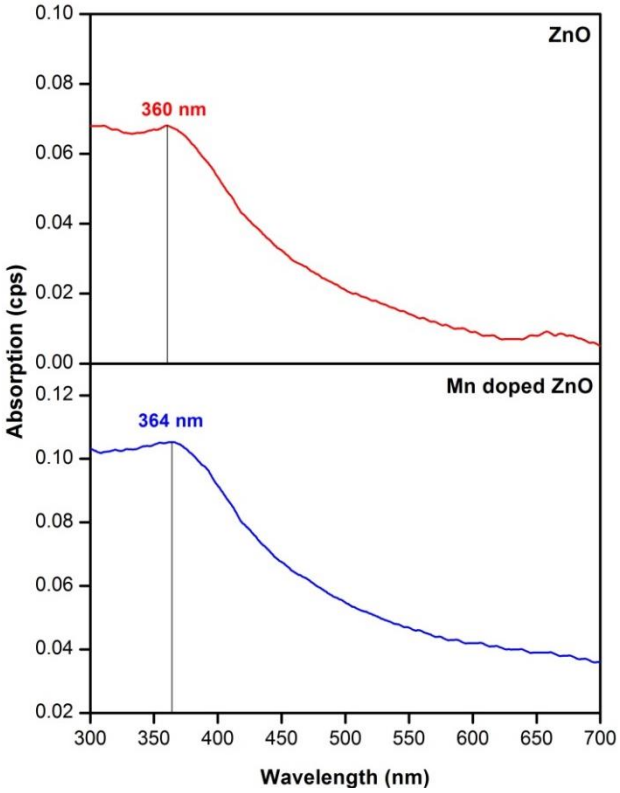

Fig.2. UV spectra of ZnO and Mn doped ZnO

The position of the absorption spectra is observed to shift towards the higher wavelength side due to Mn doped concentration in ZnO. This indicates that the band gap of ZnO material decreases with the doping concentration of Mn^{2+} ion. The decrease in the band gap or red shift can be explained by the negative Burstein–Moss effect. This is the phenomenon that the Fermi level merges into the conduction band width increase of the carrier concentration. The red shift in the absorption spectra depicts the incorporation of Mn inside the ZnO lattice. It may be due to the Micro strain due to Mn doping which cause a change in band structure of doped ZnO resulting in red shift [10]. The band gap energy can be determined using the formula:

$$E_g = \frac{hc}{\lambda} \qquad (9)$$

Where, E_g – Energy gap, h- Planck`s Constant, c- Velocity of light, λ – Wavelength.

3.3. FTIR Analysis

Fig.3 illustrates the FTIR Spectra of green synthesized ZnO and Mn doped ZnO nanoparticles using Carica Papaya extract. Fourier Transform Infrared Spectroscopy of ZnO and Mn doped ZnO a nanoparticle has been used to determine the presence of vibrational bands in the prepared samples.

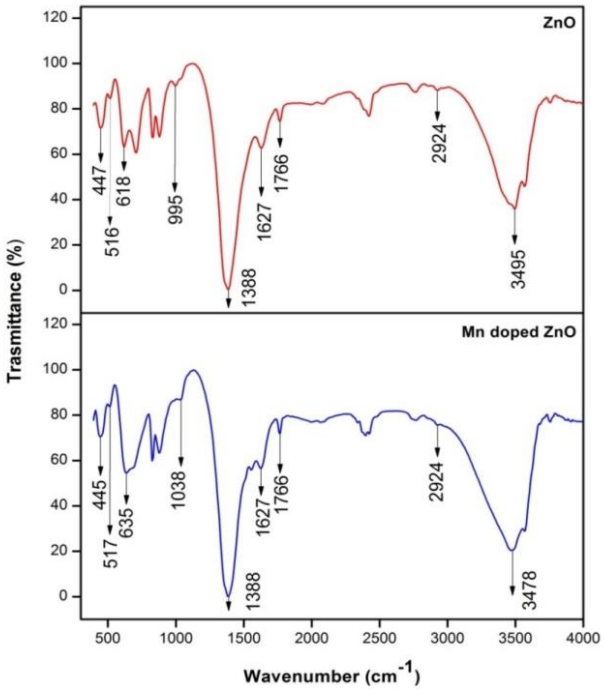

Fig.3. FTIR spectra of ZnO and Mn doped ZnO

Normally, the FTIR spectra give information about the presence of functional groups, molecular geometry and inter- or intra molecular interactions in the prepared samples. It depicts a sequence of absorption bands in a sort of 400 and 4000 cm^{-1}. The peaks in the range 600-800 cm^{-1} of FTIR spectra of Mn doped ZnO broadened when compared it with Pure ZnO, which is due to the presence of Mn^{2+} ions. In the spectra of ZnO, the characteristic vibration peaks at 447 and 516 cm^{-1} due to the vibration of Zn and O atoms in ZnO [15]. The bands observed at 618 cm^{-1} correspond to Zn–O bond, which confirms the presence of end product [3]. The peak at 995 cm^{-1} is associated with the strong C=C bending. The peaks at 1388 and 1627 cm^{-1} are attributed to the medium bending of C-H and

strong stretching of C=C of the sample, respectively. The appearance of peak at 1766 cm^{-1}, 2924 cm^{-1} and 3495 cm^{-1} in fig.3 is may be due to the strong C=O stretching, medium C-H stretching and strong O-H stretching due to the water present in the ZnO nanoparticles [16]. On the other hand, the FTIR spectra of Mn doped ZnO nanoparticle is almost same as the spectra of ZnO, except the vibrational peaks at 445 cm^{-1}, 517 cm^{-1} and 635 cm^{-1} which corresponds to the vibration of Zn and O atoms in ZnO and the formation of Mn doped ZnO nanoparticles. Table 3 shows different vibration modes of Carica Papaya ZnO and Mn doped ZnO end product. In general, papaya leaf extract has the various phytochemical components like flavonoids, phenols etc. These components can act as both capping and reducing agent that are strongly attached on the surface of Zn precursors.

Table 3. FTIR vibration frequencies for different modes of ZnO and Mn-doped Zn

ZnO	Mn doped ZnO	Vibrational modes
447	445	Zn
516	517	O
618	635	Zn-O
995	1038	Strong C=C bending
1388	1388	Medium bending of C-H
1627	1627	Strong stretching of C=C
1766	1766	Strong C=O stretching
2924	2924	Medium C-H stretching
3495	3478	Strong O-H stretching

3.4. Antibacterial Activity

The antibacterial activity of pure, Mn doped green synthesis ZnO nanoparticles and antibiotic (Gentamicin) are investigated against Gram positive and Gram-negative pathogenic bacteria's such as *E. coli* and S. *aureus* using agar well diffusion method. The results in table 4 and table 5 showed that the synthesized ZnO and Mn doped ZnO nanoparticles expressed anti-bactericidal activity against the both Gram negative and Gram-positive bacteria.

From fig.4 and fig.5, it is noted that Mn doped ZnO samples prevented the growth of bacteria's remarkably and formed well-defined zones around the samples. The increase in the zone of inhibition in Mn doped ZnO sample is caused by the substitution of Mn ions into the Zn ion sites. Moreover, increase in concentration (25µL, 50µL, 75µL) can also enhance the increase in the Zone of inhibition is noted in fig.6 and fig.7.

The negative control could not exhibit any zone of inhibition. ZnO and Mn doped ZnO exhibited remarkable antibacterial activity against all tested bacterial strains. Gentamicin was used as reference drug. The following tables show the antibacterial activities of Mn doped ZnO against tested organisms.

Table 4. Antibacterial activity of ZnO nanoparticles

Test Organisms	Diameter of Zone of Inhibition (mm)			
	25 µL	**50 µL**	**75 µL**	**Positive Control**
E. *coli*	20	23	25	21
S. *aureus*	18	21	23	16

Table 5. Antibacterial activity of Mn doped ZnO nanoparticles

Test Organisms	Diameter of Zone of Inhibition (mm)			
	25µL	**50µL**	**75 µL**	**Positive Control**
E. *coli*	24	27	28	16
S. *aureus*	21	25	27	21

The antibacterial activity of the ZnO nanoparticles may be related to several mechanisms including the generation of reactive oxygen species (ROS) on the surface of the particles, release of Zn^{2+} ions from the ZnO samples and the penetration of these nanoparticles which contributes to the mechanical destruction of cell membrane. The hydroxyl radicals and superoxide anions are negatively charged and hence they cannot penetrate into the cell membrane, but they can cause fatal damage to proteins, Deoxyribonucleic acid and lipids, whereas, H_2O_2 can penetrate directly into the cell wall and kill the bacteria [17].

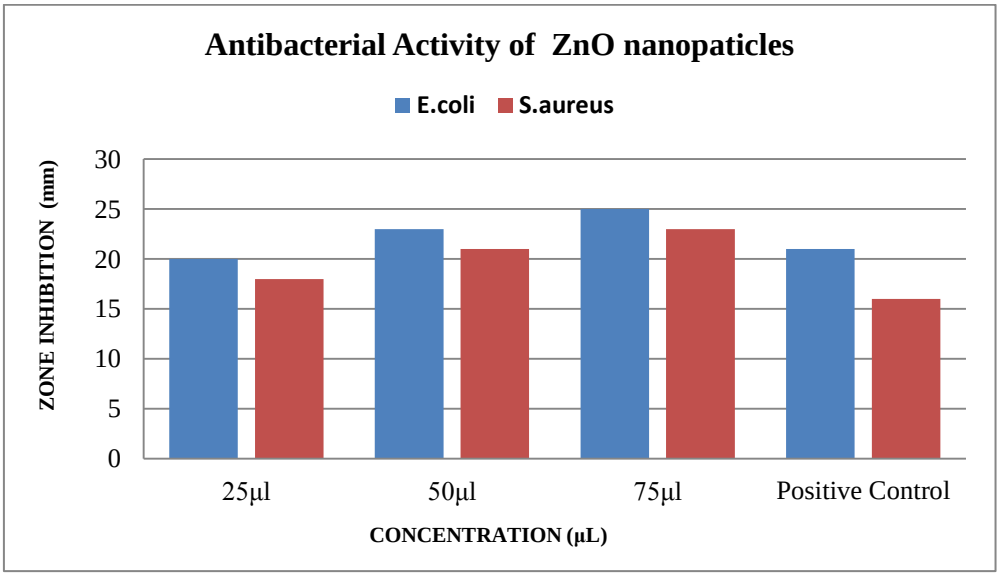

Fig.4. The Inhibition zones caused by ZnO nanoparticles against *E. coli* and *S. aureus*

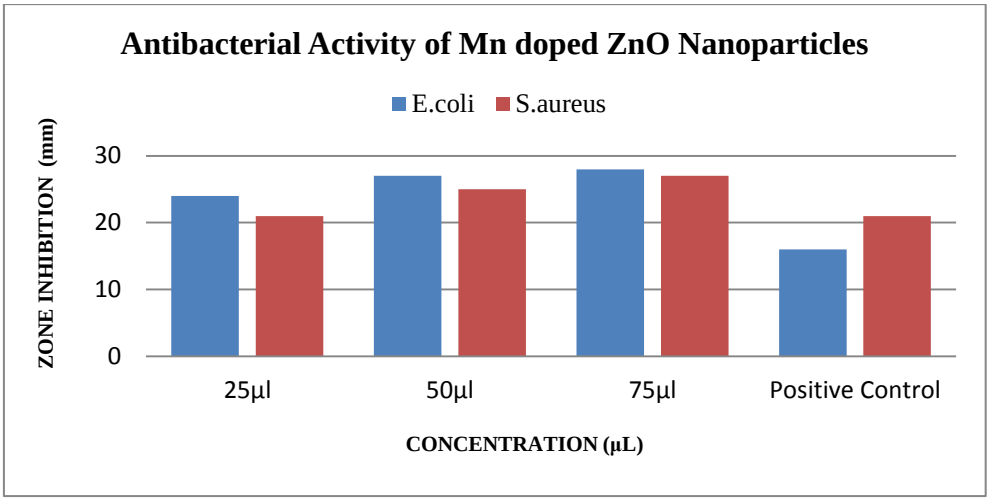

Fig.5. The Inhibition zones caused by Mn doped ZnO nanoparticles against E. coli and S. aureus

These results showed the Mn doped ZnO nanoparticles have more potential antibacterial effect on Gram negative bacteria than Gram positive bacteria. The dopant (Mn) enhances the antibacterial activity of ZnO over *Escherichia coli* and *Staphylococcus aureus* which is evident from the following graphs.

Fig.6. Antibacterial activity of ZnO nanoparticles against *E. coli and* S. *aureus*

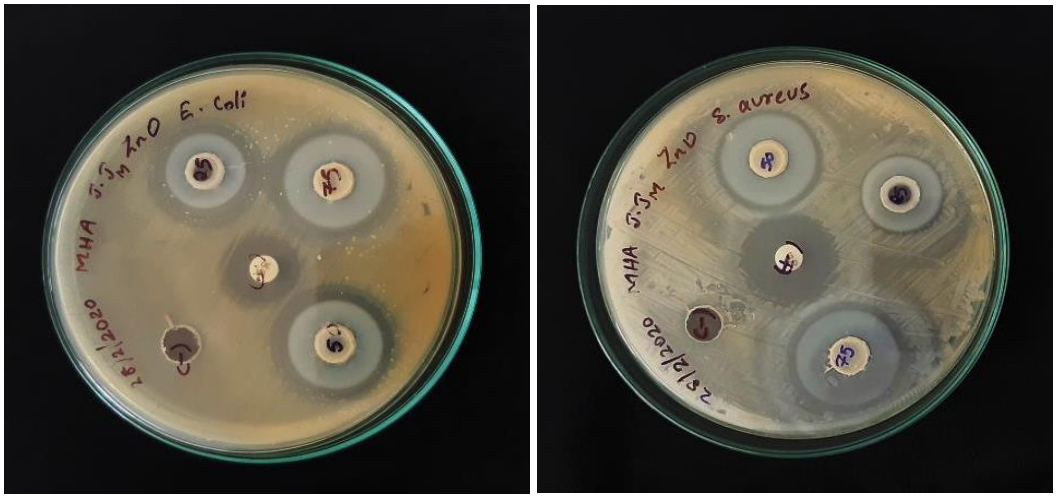

Fig.7. Antibacterial activity of Mn doped ZnO nanoparticles against *E. coli and* S. *aureus*

These results showed the Mn doped ZnO nanoparticles have more potential antibacterial effect on Gram negative bacteria than Gram positive bacteria. The dopant (Mn) enhances the antibacterial activity of ZnO over *Escherichia coli* and *Staphylococcus aureus* which is evident from the following graphs.

4. Conclusion

In the present work, green synthesis using Carica Papaya extract with ZnO and Mn-doped ZnO nanoparticles with hexagonal crystal structure were synthesized by co-precipitation method. Results of XRD analysis revealed average crystalline size of 7.75 and 8.49 nm for ZnO and Mn-doped ZnO nanoparticles.

The absorption studies confirmed the existence of manganese at zinc sites in Mn-doped ZnO nanoparticles. UV–Vis studies revealed that the optical band-gap energy is 3.41 and 3.45 eV for ZnO and Mn-doped ZnO nanoparticles respectively. FTIR analysis also confirms the presence of Mn dopant through the peak shifting from 618 cm^{-1} to 635 cm^{-1}. The Mn-doped ZnO nanoparticles show better antibacterial activity against the *E. coli* bacteria than against others when doping level is higher (5 wt%) and duration of time is longer.

This better antibacterial efficiency at higher doping levels is due to the interstitial incorporation of Mn and Zn, the resultant increase in the carrier concentration and the increase in the crystallite size as evidenced by XRD results.

Declarations

Source of Funding

This research was funded by DST-FIST scheme of Dr. N.G.P Arts and Science college (Communication number - Dr.NGPASC 2021-22 BAS006).

Competing Interests Statement

The authors declare no competing financial, professional and personal interests.

Consent for publication

Authors declare that they consented for the publication of this research work.

References

[1] V. N. Kalpana and V. Devi Rajeswari, "A Review on Green Synthesis, Biomedical Applications, and Toxicity Studies of ZnO NPs," Bioinorg. Chem. Appl., vol. 2018, 2018, doi: 10.1155/2018/3569758.

[2] S. Fakhari, M. Jamzad, and H. Kabiri Fard, "Green synthesis of zinc oxide nanoparticles: a comparison," Green Chem. Lett. Rev., vol. 12, no. 1, pp. 19–24, 2019, doi: 10.1080/17518253.2018.1547925.

[3] Gil otis, Michal Ejgenberg and Yitzhak Mastai, "Solvent free mechanochemical synthesis of ZnO nanoparticles by high energy ball milling of $eZn(OH)_2$ crystals", Nanomaterials, Vol.11, No.1 pp-238, 2021. doi: 10.3390/nano11010238.

[4] K. Pradeev raj et al., "Influence of Mg Doping on ZnO Nanoparticles for Enhanced Photocatalytic Evaluation and Antibacterial Analysis," Nanoscale Res. Lett., vol. 13, 2018, doi: 10.1186/s11671-018-2643-x.

[5] A. Kolodziejczak-Radzimska and T. Jesionowski, "Zinc oxide-from synthesis to application: A review," Materials (Basel)., vol. 7, no. 4, pp. 2833–2881, 2014, doi: 10.3390/ma7042833.

[6] N. Bala et al., "Green synthesis of zinc oxide nanoparticles using Hibiscus subdariffa leaf extract: Effect of temperature on synthesis, anti-bacterial activity and anti-diabetic activity," RSC Adv., vol. 5, no. 7, pp. 4993–5003, 2015, doi: 10.1039/c4ra12784f.

[7] G.K Prashanth et al., "Effect of doping and UV exposure on the antibacterial, anticancer and ROS generation activities of zinc oxide nanoparticles", Journal of asian ceramic societies, Vol.8, No.4, pp. 1175-1187, 2020. doi: 10.1080/21870764.2020.1824328.

[8] N.Priyadharsini, M.Thamilselvan, S.Sangeetha and S.Vairam, "Effect of Neodymium substitution on structural, optical, magnetic and antibacterial activity of Zince Selenide nanoparticles," Journal of Ovonic research, Vol.12, No.2, pp.87-93, 2016.

[9] G.K Prashanth et al., "Comparison of antimicrobial, antioxidant and anticancer activities of ZnO nanoparticles prepared by lemon juice and citric acid fueled solution combustion synthesis", Bionanoscience, 9, 799-812, 2019.

[10] A.Abu El-Fadl, Ragaa S.Mahmoud, A.A.Abu Sehly, El Sayed Yousel, "The role of Co in doping ZnO nano particles in enchancement the structural, optical and magnetic properties for spintronics", Journal of Ovonic research, Vol.17, No.6, pp.499-507, 2021.

[11] R. K. Sharma, S. Patel, and K. C. Pargaien, "Synthesis, characterization and properties of Mn-doped ZnO nanocrystals," Adv. Nat. Sci. Nanosci. Nanotechnol., vol. 3, no. 3, 2012, doi: 10.1088/2043-6262/3/3/035005.

[12] T. L. Tan, C. W. Lai, and S. B. Abd Hamid, "Tunable band gap energy of Mn-doped ZnO nanoparticles using the coprecipitation technique," J. Nanomater., vol. 2014, 2014, doi: 10.1155/2014/371720.

[13] E. H. K. Ikram, R. Stanley, M. Netzel, and K. Fanning, "Phytochemicals of papaya and its traditional health and culinary uses - A review," J. Food Compos. Anal., vol. 41, pp. 201–211, 2015, doi: 10.1016/j.jfca.2015.02.010.

[14] N. A. Imaga et al., "Phytochemical and antioxidant nutrient constituents of Carica papaya and parquetina nigrescens extracts," Sci. Res. Essays, vol. 5, no. 16, pp. 2201–2205, 2010.

[15] K. Rekha, M. Nirmala, M. G. Nair, and A. Anukaliani, "Structural, optical, photocatalytic and antibacterial activity of zinco xide and manganese doped zinc oxide nanoparticles," Phys. B Condens. Matter, vol. 405, no. 15, pp. 3180–3185, 2010, doi: 10.1016/j.physb.2010.04.042.

[16] R. Rathnasamy, P. Thangasamy, R. Thangamuthu, S. Sampath, and V. Alagan, "Green synthesis of ZnO nanoparticles using Carica papaya leaf extracts for photocatalytic and photovoltaic applications," J. Mater. Sci. Mater. Electron., vol. 28, no. 14, pp. 10374–10381, 2017, doi: 10.1007/s10854-017-6807-8.

[17] A. Dhanalakshmi, B. Natarajan, V. Ramadas, A. Palanimurugan, and S. Thanikaikarasan, "Structural, morphological, optical and antibacterial activity of rod-shaped zinc oxide and manganese-doped zinc oxide nanoparticles," Pramana - J. Phys., vol. 87, no. 4, 2016, doi: 10.1007/s12043-016-1248-0.

[18] Saka Abel, Jule Leta Tesfaye, Nagaraj Nagaprasad, R.Shanugam, L.Priyanka Dwarampudi and R Krishnaraj, "Synthesis and Characterization of zinc oxide nanoparticles using moringa leaf extract", Journal of nanomaterials, Vol.2021, pp. 6, 2021. doi:10.1155/2021/4525770.

[19] L. Umaralikhan and M. J. M. Jaffar, "Green synthesis of ZnO and Mg doped ZnO nanoparticles, and its optical properties," J. Mater. Sci. Mater. Electron., vol. 28, no. 11, pp. 7677–7685, 2017, doi: 10.1007/s10854-017-6461-1.

[20] T. Bhuyan, K. Mishra, M. Khanuja, R. Prasad, and A. Varma, "Biosynthesis of zinc oxide nanoparticles from Azadirachta indica for antibacterial and photocatalytic applications," Mater. Sci. Semicond. Process., vol. 32, pp. 55–61, 2015, doi: 10.1016/j.mssp.2014.12.053.

[21] G. K Prashanth, P A Prashanth, B M Nagabhushana, S.Ananda etal, "Comparison of anticancer activity of biocompatible ZnO nanoparticles prepared by solution combution synthesis using aqueous leaf extracts of Abutilon indicum, Melia azedarach and Indigofera tinctoria as bio fuels", Artificial cells, Nanomedicine and Biotechnology, Vol. 46, No.5, pp.968-979, 2018. doi: 10.1080/21691401.2017.1351982.

[22] G.K Prashanth et al., "Antitubercular activity of Zno nanoparticles prepared by solution combution synthesis using lemon juice as bio fuel", Materials science and Engineering:C, Vol. 75, No.1, pp 1026-1033, 2017. doi: 10.1016/j.msec.2017.02.093.

[23] M. Sathya and K. Pushpanathan, "Synthesis and Optical Properties of Pb Doped ZnO Nanoparticles," Appl. Surf. Sci., vol. 449, pp. 346–357, 2018, doi: 10.1016/j.apsusc.2017.11.127

[24] Mahla Deylam, Effat Alizadeh, Manizheh Sarikhani, and Masoumeh Firouzamandi, "Zinc oxide nanopaticles promote the aging process in a size- dependent manner", Journal of materials science: Materials in medicine, Vol. 32, 128, 2021. doi: 10.1007/s10856-021-06602-x.

[25] X.Y Lim, J.S.W.Chan, N.Japri, J.C.Lee and T.Y.C. Tan, "Carica papaya L.Leaf: A systematic scoping review on biological safety and herb drug interactions", Evidence based complementary and alternative medicine, Vol 2021, pp.21, 2021. doi: 10.1155/2021/5511221.

[26] Antonia windkouni bere etal., "Carica papaya leaf extract silver synthesized nanoparticles inhibit dengue type 2 viral replication in vitro", Pharmaceuticals, Vol.14, No.8, pp.718, 2021. doi: 10.3390/ph14080718.